Title

C1q-targeted monoclonal antibody prevents complement-dependent cytotoxicity and neuropathology in in vitro and mouse models of neuromyelitis optica

Journal

Acta Neuropathologica, 125(6)

ISSN

0001-6322

Authors

Phuan, Puay-Wah
Zhang, Hua
Asavapanumas, Nithi
et al.

Publication Date

2013-06-01

DOI

10.1007/s00401-013-1128-3

Peer reviewed

Published in final edited form as:
Acta Neuropathol. 2013 June ; 125(6): 829–840. doi:10.1007/s00401-013-1128-3.

C1q-targeted monoclonal antibody prevents complement-dependent cytotoxicity and neuropathology in in vitro and mouse models of neuromyelitis optica

Puay-Wah Phuan,
Departments of Medicine and Physiology, University of California, 1246 Health Sciences East Tower, San Francisco, CA 941143-0521, USA, URL: http://www.ucsf.edu/verklab

Hua Zhang,
Departments of Medicine and Physiology, University of California, 1246 Health Sciences East Tower, San Francisco, CA 941143-0521, USA, URL: http://www.ucsf.edu/verklab

Nithi Asavapanumas,
Departments of Medicine and Physiology, University of California, 1246 Health Sciences East Tower, San Francisco, CA 941143-0521, USA, URL: http://www.ucsf.edu/verklab

Michael Leviten,
Annexon, Inc, Palo Alto, CA, USA

Arnon Rosenthal,
Annexon, Inc, Palo Alto, CA, USA

Lukmanee Tradtrantip, and
Departments of Medicine and Physiology, University of California, 1246 Health Sciences East Tower, San Francisco, CA 941143-0521, USA, URL: http://www.ucsf.edu/verklab

A. S. Verkman
Departments of Medicine and Physiology, University of California, 1246 Health Sciences East Tower, San Francisco, CA 941143-0521, USA, URL: http://www.ucsf.edu/verklab

A. S. Verkman: Alan.Verkman@ucsf.edu

Abstract

Neuromyelitis optica (NMO) is an autoimmune disorder with inflammatory demyelinating lesions in the central nervous system, particularly in the spinal cord and optic nerve. NMO pathogenesis is thought to involve binding of anti-aquaporin-4 (AQP4) autoantibodies to astrocytes, which causes complement-dependent cytotoxicity (CDC) and downstream inflammation leading to oligodendrocyte and neuronal injury. Vasculocentric deposition of activated complement is a prominent feature of NMO pathology. Here, we show that a neutralizing monoclonal antibody against the C1q protein in the classical complement pathway prevents AQP4 autoantibody-dependent CDC in cell cultures and NMO lesions in ex vivo spinal cord slice cultures and in mice. A monoclonal antibody against human C1q with 11 nM binding affinity prevented CDC caused by NMO patient serum in AQP4-transfected cells and primary astrocyte cultures, and prevented complement-dependent cell-mediated cytotoxicity (CDCC) produced by natural killer cells. The anti-C1q antibody prevented astrocyte damage and demyelination in mouse spinal cord slice cultures exposed to AQP4 autoantibody and human complement. In a mouse model of NMO produced by

Correspondence to: A. S. Verkman, Alan.Verkman@ucsf.edu.

Conflict of interest Drs. Leviten and Rosenthal are employed by Annexon, Inc.

intracerebral injection of AQP4 autoantibody and human complement, the inflammatory demyelinating lesions were greatly reduced by intracerebral administration of the anti-C1q antibody. These results provide proof-of-concept for C1q-targeted monoclonal antibody therapy in NMO. Targeting of C1q inhibits the classical complement pathway directly and causes secondary inhibition of CDCC and the alternative complement pathway. As C1q-targeted therapy leaves the lectin complement activation pathway largely intact, its side-effect profile is predicted to differ from that of therapies targeting downstream complement proteins.

Keywords

NMO; Aquaporin-4; Complement; Neuroinflammation; Autoimmunity

Introduction

Neuromyelitis optica (NMO) is an autoimmune disease of the central nervous system in which inflammatory demyelinating lesions cause motor and visual impairment [17, 18, 58]. Serum autoantibodies against astrocyte water channel aquaporin-4 (AQP4), called NMO-IgG [26], are found in most NMO patients [19]. NMO pathogenesis is thought to involve NMO-IgG binding to AQP4, causing astrocyte cytotoxicity with secondary inflammation leading to oligodendrocyte injury, demyelination and neuron loss [22, 32]. NMO therapies used at present include immunosuppressive drugs, B cell depletion by rituximab, and plasma exchange [13, 21].

There is compelling evidence for a central role of complement in NMO pathogenesis. Vasculocentric deposition of activated complement is a prominent feature of neuroinflammatory lesions in NMO [14, 27, 30, 41]. NMO-IgG is an immunoglobulin G subtype 1 autoantibody that causes complement-dependent cytotoxicity (CDC) in vitro in AQP4-expressing cells, including astrocytes [4, 15, 16, 44]. Characteristic NMO pathology, with loss of AQP4 and glial fibrillary acid protein (GFAP) immunoreactivity and demyelination, is produced ex vivo in spinal cord and optic nerve slice cultures exposed to NMO-IgG and human complement [62]. NMO pathology is produced in mice in vivo administered NMO-IgG and human complement by intracerebral injection or infusion [42, 43, 63]. A small, open-label trial of eculizumab, a monoclonal antibody inhibitor of C5 convertase in the classical complement pathway [33, 40], showed benefit in NMO, reducing the recurrence rate in NMO patients with severe disease [35].

Here, we evaluated the potential efficacy in NMO of a monoclonal antibody that neutralizes the activity of human complement protein C1q. As C1q is the first component in the classical complement pathway that binds to the Fc portion of AQP4-bound NMO-IgG, its inhibition would protect against downstream proteins in the classical complement pathway [38, 52], preventing formation of the C5b-9 membrane attack complex and hence CDC. In addition, C1q inhibition would prevent complement-dependent cell-mediated cytotoxicity (CDCC), which involves the actions of C3 and C5-derived anaphylatoxins on chemotaxis, IgG binding and cytotoxic action of effector leukocytes [24]. CDCC is probably an important mechanism of NMO pathogenesis as demonstrated by reduced pathology mouse models of NMO where neutrophil and/or eosinophil function is inhibited by antibodies or drugs [43, 63]. C1q inhibition would also inhibit antibody-dependent cytotoxicity that is initiated by C1q binding in the classical pathway and amplified by the alternative complement pathway. We show here that an anti-C1q monoclonal antibody is effective in preventing cytotoxicity and NMO pathology in cell culture, ex vivo organ culture and in vivo mouse models of NMO.

Materials and methods

Cell culture and NMO antibodies

Human M23-AQP4 expressing Chinese hamster ovary (CHO) cells were generated by stable transfection, as described [34]. CHO cells were cultured in F-12 Ham's Nutrient mix medium supplemented with 10 % fetal bovine serum, 100 U/ml penicillin, and 100 μg/ml streptomycin. Geneticin (200 μg/ml) was used as selection marker. Cells were grown at 37 °C in 5 % CO_2/95 % air. Recombinant monoclonal NMO antibodies (rAb-53) were generated from clonally-expanded plasma blasts from cerebrospinal fluid (CSF) of NMO patients and purified as described [4]. Isotype-matched controls antibodies included a non-NMO rAb (rAb-2B4) against measles virus nucleocapsid protein, and mouse IgG1 kappa monoclonal (ab18447) from Abcam (Cambridge, MA, USA). NMO serum was obtained from NMO-IgG seropositive individuals who met the revised diagnostic criteria for clinical disease [59]. Non-NMO human serum was used as control. Purified C1q protein and C1q-depleted serum were purchased from Complement Technology Inc. (Tyler, TX, USA).

C1q and C1s antibodies

Mouse monoclonal antibodies against C1q ($C1q^{mAb}$) and C1s (two antibodies: $C1s^{mAb1}$, $C1s^{mAb2}$) were generated and purified as follows. The anti-C1q antibody 4A4B11 hybridoma line was acquired from ATCC (ATCC HB-8327TM). The anti-C1s antibodies are mouse IgG1 antibodies generated by immunizing mice with purified human C1s (Complement Technology Inc., Tyler, TX, USA) and screening hybridomas for reactivity to the immunizing protein. Female BALB/c mice were injected intraperitoneally with 25 mg protein in complete Freund's adjuvant on day 0 and boosts were done with 25 mg of C1s in incomplete Freund's adjuvant on days 21, 42, 52, and a final intravenous boost on day 63. Four days following the final boost the mice were euthanized, spleens removed, and splenocytes were fused with the myeloma cell line SP2/0. Fused cells were grown on hypoxanthine-aminopterin-thymidine (HAT) selective semi-solid media for 10–12 days and the resulting hybridomas clones were transferred to 96-well tissue culture plates and grown in HAT medium. The antibody-rich supernatants were isolated and tested in an ELISA assay for reactivity against C1s enzyme, C1s proenzyme and human transferrin (as negative control). Positive clones were isotyped and cultured for 32 days (post-HAT selection) to identify stable expressing clones. Two antibodies recognized both the C1s proenzyme and processed C1s enzyme with similar affinities and did not cross-react with C1r or transferrin. The hybridomas were expanded to generate 5 l of conditioned media. Antibodies were purified using Protein A under low endotoxin conditions, exchanged into a phosphate-buffered saline (PBS) buffer, and their concentration and purity was determined by spectrophotometry and SDS-PAGE.

Complement-dependent cytotoxicity

M23-AQP4-expressing CHO cells were plated onto 96-well microplates (Costar, Corning Inc., Corning, NY, USA) at 20,000 cells/well and grown at 37 °C/5 % CO_2 for 18–24 h. Cells were washed with PBS and incubated at room temperature for 30 min with 50 μl of rAb-53 or heat-inactivated NMO serum in live cell buffer (PBS containing 6 mM glucose and 1 mM sodium pyruvate). A solution containing pooled normal human complement serum (Innovative Research, Novi, MI, USA) and anti-C1 antibody was incubated on ice for 30 min before added to the CHO cells. Some experiments were done using purified C1q and C1q-depleted serum in which specified quantities of C1q were added to C1q-depleted serum. For studies of the alternative complement pathway, C1q-depleted or factor-B depleted serum (Quidel, Inc., San Diego, CA, USA) was used instead of normal serum. In some experiments, 100 μg/ml neutralizing anti-factor B antibody (R&D Systems, Inc., Minneapolis, MN, USA) was incubated with normal serum 30 min prior to CDC assay.

After addition of human complement, rAb-53 or heat-inactivated NMO serum and anti-C1 antibody, cells were incubated for 60 min at 27 °C, washed once with PBS, and incubated with 50 μl of a 20 % AlamarBlue solution for 45 min at 27 °C. Cytotoxicity was measured from resorufin fluorescence using a TECAN Infinite M1000 plate reader (TECAN Groups Ltd, Mannedorf, Switzerland) (excitation/emission 560/590 nm). For live/dead cells staining, cells were washed with PBS and then incubated with 1 μM calcein-AM (live cells, green fluorescence) and 2 μM ethidium homodimer-1 (dead cells, red fluorescence) (Invitrogen) in PBS for 15 min prior to imaging.

Antibody-dependent cell-mediated cytotoxicity (ADCC)

M23-AQP4-expressing CHO cells on 96-well microplates (as for CDC) were washed with PBS and incubated for 1 h at 37 °C with rAb-53 (1 and 10 μg/ml) or control-rAb, and NK cells overexpressing CD16 (Conkwest, San Diego, CA, USA) as effector cells at an effector:target cell ratio of 20:1, with or without $C1q^{mAb}$. Wells were washed gently five times with PBS to remove NK cells before addition of 50 μl of 20 % AlamarBlue solution. Cells were incubated for 45 min at 27 °C and cytotoxicity was determined from resorufin fluorescence.

Complement-dependent cell-mediated cytotoxicity

M23-AQP4-expressing CHO cells on 96-well microplates were washed with PBS and incubated for 1 h at 37 °C with rAb-53 (0.25 μg/ml), 1 % human complement and NK cells (effector:target cell ratio 20:1), with or without 2.5 μg/ml $C1q^{mAb}$. Wells were washed to remove NK cells and cytotoxicity was measured as above.

Surface plasmon resonance

Surface plasmon resonance (SPR) measurements were done on a Biacore T100 instrument (GE Healthcare, Pis-cataway, NJ, USA). Purified C1q protein was diluted with 10 mM MES buffer (pH 6.5) to 10 μg/ml and immobilized onto the surface of a carboxymethylate-functionalized CM5 sensor chip (GE Healthcare) using standard carbodiimide coupling. Unreacted surface was blocked by injection of 1 M ethanolamine-HCl. The reference control flow cell was coupled with 1 M ethanolamine-HCl only. Binding was measured at 25 °C using pH 7.4 Hepes-buffered saline as running buffer at a flow rate of 20 μl/min. $C1q^{mAb}$ and a control mouse IgG1 antibody in identical buffer were injected for 180 s over sensor chip followed by a 300 s washout period at the same flow rate. Sensorgrams were corrected by subtraction of responses of the unloaded reference flow cell. Equilibrium constants for antibody-antigen binding were determined using a 1:1 Langmuir binding-affinity model.

NMO-IgG binding

M23-AQP4-expressing CHO cells were plated onto 96-well microplates and grown for 18–24 h to confluence. Cells were washed twice with PBS and blocked with 1 % bovine serum albumin (BSA) in PBS for 30 min. After removal of blocking solution, a premixed solution (10 μl) of rAb-53 (1.5 μg/ml) and horseradish peroxidase (HRP)-labeled goat anti-human IgG secondary antibody (1:500 dilution; Invitrogen) was added. Following 1 h incubation at room temperature, cells were washed three times with PBS containing 0.05 % Tween-20, and HRP activity was assayed by addition of 50 μl Amplex Red substrate (100 μM, Sigma) and 2 mM H_2O_2 as described [50]. Fluorescence was measured after 10 min (excitation/emission 540/590 nm).

Immunofluorescence

Cells were grown on glass coverslips for 24 h and then washed with PBS and incubated for 30 min in live cell blocking buffer (PBS containing 6 mM glucose, 1 mM sodium pyruvate,

1 % BSA). Cells were incubated for 60 min with rAb-53 in blocking buffer at a final concentration of 1 μg/ml. Cells were then rinsed in PBS, fixed in 4 % paraformaldehyde for 15 min, and permeabilized with 0.1 % Triton X-100. Cells were incubated for 60 min with 0.4 μg/ml polyclonal, C-terminal specific rabbit anti-AQP4 antibody (H-80, Santa Cruz Biotechnology, Santa Cruz, CA, USA) and then for 30 min with 4 μg/ml goat anti-human IgG-conjugated Alexa Fluor 488 and 4 μg/ml goat anti-rabbit IgG-conjugated Alexa Fluor 555 (Invitrogen) in blocking buffer, as described [7]. Red and green fluorescence was imaged on a Nikon Eclipse TE2000S inverted epifluorescence microscope (Nikon, Melville, NY, USA).

Ex vivo spinal cord slice model of NMO

Transverse slices of cervical spinal cord from 7-day old CD1 mice were cut at 300-μm thickness using a vibratome and placed in ice-cold Hank's balanced salt solution (HBSS, pH 7.2), as described [62]. All animal studies were approved by the UCSF Committee on Animal Research. Slices were placed on transparent membrane inserts (Millipore, Millicell-CM 0.4 μm pores, 30 mm diameter) in 6-well plates containing 1 ml culture medium, with a thin film of culture medium covering the slices. Slices were cultured in 5 % CO_2 at 37 °C for 7 days in 50 % MEM, 25 % HBSS, 25 % horse serum, 1 % penicillin–streptomycin, 0.65 % glucose and 25 mM HEPES. Slices were then incubated with rAb-53 (10 μg/mL) and human complement (5 %) with or without C1qmAb (2.5 μg/mL) for 24 h. Slices were cultured for an additional 24 h, and immunostained for AQP4 and GFAP. Sections were scored as follows: 0, intact slice with normal GFAP and AQP4 staining; 1, mild astrocyte swelling and/or reduced AQP4 staining; 2, at least one lesion with loss of GFAP and AQP4 staining; 3, multiple lesions affecting >30 % of slice area; 4, lesions affecting >80 % of slice area.

In vivo intracerebral injection model of NMO

Adult CD1 mice (30–35 g) were anesthetized with 2,2,2-tri-bromoethanol (125 mg/kg intraperitoneally) and mounted in a stereotaxic frame. Following a midline scalp incision, a burr hole of diameter 1 mm was made 2 mm to the right of the bregma. A 30-gauge needle attached to 50 μl gas-tight glass syringe was inserted 3 mm deep, as described [42], to infuse 0.9 μg of rAb-53, 3 μl of human complement (with or without) 1.3 μg $C1q^{mAb}$ in a total volume of 8 μl (at 2 μl/min). 3 μl of human complement and 1.3 μg $C1q^{mAb}$ (total volume of 8 μl) was injected as a control. After 3 days mice were anesthetized and perfused through the left cardiac ventricle with 5 ml PBS and then 20 ml PBS containing 4 % PFA. Brains were post-fixed for 2 h in 4 % PFA. 5-mm thick paraffin sections were immunostained for AQP4, GFAP and MBP, as described [36]. Data are presented as percentage of immunonegative area, as defined by hand and quantified using ImageJ, normalized to total area of hemibrain slice.

Statistical analysis

Data are presented as mean ± SEM. Statistical comparisons were made using Student's *t* test.

Results

C1 monoclonal antibodies inhibit NMO-IgG- and complement-dependent cytotoxicity

CDC caused by NMO-IgG binding to AQP4 was measured in AQP4-expressing cell cultures, in which human complement was incubated for 30 min with monoclonal antibodies against C1q ($C1q^{mAb}$) or C1s ($C1s^{mAb1}$, $C1s^{mAb2}$) prior to addition to cells. Cytotoxicity was assayed using the AlamarBlue assay. Figure 1a (left) shows that $C1q^{mAb}$, $C1s^{mAb1}$ and

$C1s^{mAb2}$ prevented CDC in a concentration-dependent manner in cells exposed to the monoclonal NMO antibody rAb-53 (1.5 μg/ml) and human complement (2 % human serum). EC_{50} for each of the C1 antibodies was ~750 ng/ml. In control studies, a non-specific mouse IgG1 antibody did not prevent CDC (data not shown). Antibody efficacy was also demonstrated in a live/dead cell staining assay (Fig. 1a, right). The C1q antibody, which was further studied, was also effective in preventing CDC caused by human NMO sera. Figure 1b shows $C1q^{mAb}$ prevention of CDC in cells incubated with 2.5 % heat-inactivated sera from five different NMO patients, together with 2 % human complement. Figure 1c shows that $C1q^{mAb}$ reduced CDC in primary cultures of murine astrocytes. To produce robust CDC in astrocytes, a mutated, CDC-enhanced recombinant NMO-IgG was used because astrocytes express complement inhibitor proteins such as CD59.

Figure 1d (left) shows $C1q^{mAb}$ prevention of CDC as a function of rAb-53 concentration at fixed 2 % complement. EC_{50} was approximately independent of rAb-53 concentration, as expected. Figure 1d (right) shows CDC as a function of complement concentration at fixed rAb-53 concentration of 1.5 μg/ml. The increased EC_{50} with increasing complement is due to the greater amount of $C1q^{mAb}$ needed to neutralize the greater amount of C1q.

Characterization of $C1q^{mAb}$

Surface plasmon resonance was used to measure $C1q^{mAb}$ binding affinity to C1q. Purified C1q protein was covalently immobilized by primary amine coupling to the carboxymethylated dextran matrix of a CM5 sensor chip. Figure 2a shows C1q binding curves for different concentrations of $C1q^{mAb}$. $C1q^{mAb}$ produced a concentration-dependent increase in SPR signal, showing fast binding and very slow dissociation, which is characteristic of a high-affinity antibody-antigen binding interaction. C1q binding was not seen for a control mouse IgG1 antibody (data not shown). Using a 1:1 binding model, the dissociation constant (K_d) for $C1q^{mAb}$ binding to C1q was 11 nM.

The stoichiometry of $C1q^{mAb}$ binding to C1q was measured, which was not predictable a priori because of the multi-valency of both the antibody and antigen. $C1q^{mAb}$ is an immunoglobulin G antibody with bivalent binding sites, and C1q is a hexavalent glycoprotein containing six globular heads that are connected to a central subunit by a collagen-like strand [8, 23]. The $C1q^{mAb}$: C1q binding stoichiometry could theoretically range from 1:1 to 6:1. Figure 2b shows the $C1q^{mAb}$ concentration-dependence of CDC for different concentrations of purified C1q protein added to C1q-depleted human serum. Linear regression analysis of EC_{50} values gave a stoichiometry of ~1.5:1. Whether $C1q^{mAb}$ binds to C1q in a bivalent or monovalent manner is not determined at this point.

The kinetics of $C1q^{mAb}$ binding to C1q was measured by incubation of $C1q^{mAb}$ and complement for different times before addition to cells with rAb-53 already bound to AQP4. Figure 2c shows the time course of cytoprotection, with $t_{1/2}$ ~ 15 min under the conditions of the experiment.

As the C1 complex, which contains C1q, C1r and C1s, is the first component in the classical complement cascade pathway, we speculated that $C1q^{mAb}$ and $C1s^{mAb}$ might act in synergy to enhance cytoprotection. To investigate possible synergy, CDC was measured at different concentrations of $C1q^{mAb}$ and $C1s^{mAb1}$, each with 2 % human complement and 1.5 μg/ml rAb-53. Figure 2d shows additive effects of the antibodies, but no significant synergy.

Control studies were done to demonstrate that rAb-53 binding to M23-AQP4 is not affected by $C1q^{mAb}$. At a high $C1q^{mAb}$ concentration of 2.5 μg/ml, no effect on rAb-53 binding to AQP4 was seen as measured by immunofluorescence (Fig. 2e, left) or using a HRP-based AmplexRed assay (Fig. 2e, right).

C1q antibody inhibits complement-dependent cell-mediated cytotoxicity but not antibody-dependent cellular cytotoxicity

$C1q^{mAb}$ is not expected to inhibit antibody-dependent cellular cytotoxicity (ADCC) because ADCC, which involves binding of effector cell FcRγ receptors to the IgG1 Fc region, is C1q-independent (Fig. 3a, top). Using NK cells as effector cells, incubation of NK cells and rAb-53 in M23-AQP4-expressing CHO cells produced ADCC (Fig. 3a, bottom). Inclusion of a high concentration (2.5 μg/ml) of $C1q^{mAb}$ did not reduce cytotoxicity caused by an ADCC mechanism. As controls, incubation of NK cells with $C1q^{mAb}$ or control antibody did not produce cytotoxicity.

Complement-dependent cell-mediated cytotoxicity involves complement-dependent enhancement in effector cell recruitment, function and AQP4 binding (Fig. 3b, top). For assay of CDCC, sub-maximal rAb-53 (0.25 μg/ml) and human complement (1 %) was used, which produced little cytotoxicity (by a CDC mechanism) in the absence of effector cells (Fig. 3b, bottom). However, addition of a small number of NK cells produced significant cytotoxicity when added together with the sub-maximal rAb-53 and complement, whereas the same small number of NK cells and sub-maximal rAb-53 (without complement) did not cause cytotoxicity (by an ADCC mechanism). Inclusion of 2.5 μg/ml $C1q^{mAb}$ prevented CDCC produced by the combination of rAb-53, complement and NK cells.

The contribution of the alternative complement pathway to NMO-IgG-dependent CDC was investigated. Exposure of AQP4-expressing cells to rAb-53 and factor B-depleted serum, or to serum pre-incubated anti-factor-B antibody, showed ~2-fold reduced CDC compared to normal human complement (Fig. 3c). The alternative complement pathway thus amplifies NMO-IgG-dependent CDC initiated by C1q binding.

$C1q^{mAb}$ prevents lesion formation in an ex vivo spinal cord slice model of NMO

$C1q^{mAb}$ efficacy was tested in an ex vivo spinal cord slice culture model of NMO in which NMO-IgG and complement produces lesions with loss of GFAP, AQP4, and myelin, deposition of activated complement, and activation of microglia [62]. As diagrammed in Fig. 4a, 300 μm thick spinal cord slices were cultured for 7 days, then incubated for 24 h with rAb-53, and complement, with or without $C1q^{mAb}$, and then immunostained for AQP4 and GFAP as markers of NMO pathology. Figure 4b shows marked loss of AQP4 and GFAP immunoreactivity in spinal cord slices incubated for 24 h with 10 μg/ml rAb-53 and 5 % human complement. Figure 4c summarizes lesion scores (0, no pathology; 4, extensive pathology). Inclusion of $C1q^{mAb}$ during the 24 h incubation with rAb-53 and complement greatly reduced lesion severity. In control studies, rAb-53, complement or $C1q^{mAb}$, each alone, did not produce pathology.

$C1q^{mAb}$ prevents lesion formation in an in vivo mouse model of NMO

The efficacy of $C1q^{mAb}$ was also tested in an in vivo mouse model of NMO in which intracerebral injection of rAb-53 and human complement produces marked loss of AQP4, GFAP and myelin (Fig. 5a). Figure 5b shows a higher magnification of the lesion, showing loss of AQP4, GFAP, and myelin. The lesions are surrounded by reactive astrocytes that overexpress GFAP. Intracerebral injection of rAb-53 and human complement together with Clq^{mAb} produced little loss of AQP4, GFAP or myelin. As control, intracerebral injection of human complement and Clq^{mAb}, without rAb-53, did not cause pathology. Quantification of lesion size showed greatly reduced lesion size when $C1q^{mAb}$ was present (Fig. 5c).

Discussion

Improved therapies for NMO are needed because there is considerable morbidity and mortality, with paralysis, blindness and death, even with aggressive immunosuppression and plasma exchange [21, 45, 53, 57]. Several non-immunosuppressive therapies are under evaluation, including antibody and small-molecule blockers of NMO-IgG binding to AQP4 [50, 51] and enzymatic strategies to neutralize NMO-IgG pathogenicity [48, 49]. The anti-Il-6 receptor antibody toculizumab, which is used in rheumatoid arthritis, is under evaluation in NMO based on its action in reducing plasma cell number [3, 20]. The repurposing of various monoclonal antibodies and small molecules that target specific leukocyte types is being considered as well, including neutrophil elastase inhibitors [43] and eosinophil-stabilizing drugs [63]. Other potential strategies for new NMO therapies include reduction in cell-surface AQP4 expression or orthogonal array assembly, prevention of NMO-IgG passage across the blood–brain barrier, and upregulation of complement inhibitor proteins on astrocytes.

We showed here that inhibition of C1q, the initiating protein in the classical complement pathway, by a recombinant anti-C1q monoclonal antibody reduced cytotoxicity in AQP4-expressing CHO cells and murine astrocyte cultures exposed to complement and NMO autoantibody (Fig. 1a–c). Using NK cells as effector cells, $C1q^{mAb}$ did not prevent ADCC, which is C1q-independent (Fig. 3a). The apparent binding affinity of $C1q^{mAb}$ to C1q protein is 11 nM, which is comparable to that of various approved monoclonal antibody therapeutics, such as rituximab to its antigen CD20 (~8 nM) [37] and the glycoprotein IIb/IIIa inhibitor abciximab (~5 nM) [47]. The stoichiometry of $C1q^{mAb}$ binding to C1q, which could theoretically be in the range from 1:1 to 6:1, was determined to be ~1.5:1, which establishes the molar quantity of $C1q^{mAb}$ needed to neutralize C1q function.

$C1q^{mAb}$ reduced lesion severity in an ex vivo spinal cord slice culture model and a mouse model of NMO (Figs. 4, 5). The mouse data should be viewed cautiously as the available mouse models of NMO are somewhat artificial in that they require intracerebral injection or continuous infusion of NMO antibody and human complement [42, 63]. We were unable to demonstrate efficacy of intraperitoneally administered $C1q^{mAb}$ in mouse models, despite obtaining high serum concentration (data not shown), perhaps because of limited $C1q^{mAb}$ penetration into brain during NMO lesion formation. As discussed [32], improved animal models of NMO created by passive transfer of NMO antibody are needed, which, for testing of complement-targeted therapeutics, utilize endogenous complement. The $C1q^{mAb}$ studied here was inactive against rat complement (data not shown), precluding informative rat studies.

The reported benefit of eculizumab in a small, open-label clinical trial [35] supports the utility of complement inhibition in NMO, as does human NMO pathology, showing prominent vasculocentric complement deposition, and data from mouse models, showing NMO lesions following intracerebral injection of NMO-IgG and complement. As diagrammed in Fig. 6, C1q inhibition would be beneficial in NMO by several mechanisms. C1 inhibition prevents the generation of anaphylatoxins C3a and C5a, which are involved in CDCC by causing effector cell chemotaxis, binding and degranulation [39, 61]. Cell culture and mouse studies suggested an important role of CDCC in NMO-IgG-dependent cytotoxicity and NMO lesion formation [36, 63]. Our data here showed full protection against CDC by the C1q antibody (Fig. 3b). C1 inhibition also prevents amplification of the classical pathway by the alternative complement pathway, where C3b forms a complex with activated factor B (Bb) and properdin (P) to produce the alternative pathway C3 convertase (C3bBbP), which amplifies cytotoxicity produced by the classical pathway [55, 60]. We showed here that the alternative complement pathway amplified NMO-IgG-dependent CDC

initiated by C1q binding by ~2-fold (Fig. 3c). The data here support the conclusion, based on the known biology of complement, that C1q inhibition prevents formation of the membrane attack complex, as well as CDCC and alternative pathway amplification. In addition, C1q-targeted therapy, unlike C5-targeted therapy, does not interfere with defense against bacteria involving the lectin complement activation pathway, theoretically reducing the risk of meningococcal meningitis and other bacterial infections. Though our study was focused on NMO-IgG-dependent disease in seropositive NMO, complement-targeted therapy may also be useful in some seronegative NMO patients, perhaps those in which disease is caused by alternative autoantibodies to myelin oligodendrocyte glycoprotein, NMDA-type glutamate receptors or CV2/CRMP5 [2, 25, 28].

Our results thus support the potential efficacy of C1q-targeted monoclonal antibody therapy in NMO, though with several caveats. The potential side effect profile of chronic C1q inhibition in humans is not known. Loss-of-function mutations in C1q in humans cause systemic lupus erythematosus in >90 % of individuals with these mutations [6]. The association between C1q deficiency and lupus has been speculated to include increased infections, defective clearance of immune complexes or apoptotic cells, and inadequate tolerization of immature B cells [29]. About 25 % of C1q knockout mice developed glomerulo-nephritis with immune deposits and multiple apoptotic cell bodies [5], with many apoptotic cells also seen in mice without glomerulonephritis, suggesting that C1q deficiency causes autoimmunity by impairing the clearance of apoptotic cells. Whether long-term C1q-targeted monoclonal antibody therapy will produce transient or chronic lupus-like or other autoimmune complications remains to be seen [54]. An additional concern about the efficacy of C1q-targeted therapy in NMO is C1q secretion by astrocytes and microglia cells in brain [46], whose inhibition would require adequate penetration of C1q antibody into the CNS at active NMO lesions. Finally, as with antibody therapeutics in general, there are challenges in the generation and formulation of a humanized, non-immunogenic antibody with appropriate pharmacokinetics in humans.

C1q-targeted monoclonal antibodies have potential as therapy for other autoimmune diseases involving the classical complement pathway, such as idiopathic thrombocytopenia purpura [11], anti-neutrophil cytoplasmic autoantibody-associated vasculitides [56], myasthenia gravis [12], and potentially, in hereditary angioedema (HAE) [1, 9]. Deficiency of C1 esterase inhibitor (C1-INH), caused either by reduced production of normal C1-INH (Type I HAE) or loss-of-function mutations of C1-INH (Type II HAE), leads to inappropriate activation of multiple pathways, including the complement, contact and fibrinolytic systems. Current HAE therapies include replacement of C1-INH enzyme, the anabolic steroid danazol, the kallikrein-inhibitor ecallantide, and the bradykinin B2-receptor antagonist icatibant. C1q-targeted monoclonal antibody therapy may be useful in HAE, as well as in targeting complement-independent functions C1q, which include microglial activation, maturation of immature dendritic cells, and mast cell migration [10, 31].

In conclusion, this study provides proof-of-concept for monoclonal antibody inhibition of complement protein C1q as a potential therapeutic strategy for NMO. An anti-C1q monoclonal antibody inhibited CDC and CDCC in cell and spinal cord cultures, and in a mouse model of NMO. C1q-targeted neutralizing monoclonal antibodies may be useful during acute NMO exacerbations, as well as for chronic administration to reduce recurrence rate. Human clinical trials are needed to show efficacy of C1q-targeted antibody therapy in NMO and to compare with current therapies.

Acknowledgments

This work was supported by grants EY13574, EB00415, DK35124, HL73856, DK86125 and DK72517 from the National Institutes of Health, and a grant from the Guthy-Jackson Charitable Foundation. This work was also supported by a sponsored research agreement from Annexon Inc. (Palo Alto, CA, USA). We thank Dr. Jeffrey Bennett (Univ. Colorado Denver, Aurora, CO, USA) for providing recombinant monoclonal NMO antibody and for Accelerated Cure (Waltham, MA, USA) for providing human NMO sera.

References

1. Aberer W. Hereditary angioedema treatment options: the availability of new therapies. Ann Med. 2012; 44(6):523–529. [PubMed: 22784006]
2. Asgari N, Khorooshi R, Lillevang ST, Owens T. Complement-dependent pathogenicity of brain-specific antibodies in cerebrospinal fluid. J Neuroimmunol. 2013; 254(1–2):76–82. [PubMed: 23031833]
3. Ayzenberg I, Kleiter I, Schröder A, Hellwig K, Chan A, Yamamura T, Gold R. Interleukin 6 receptor blockade in patients with neuromyelitis optica nonresponsive to anti-CD20 therapy. JAMA Neurol. 2013; 70(3):394–397. [PubMed: 23358868]
4. Bennett JL, Lam C, Kalluri SR, Saikali P, Bautista K, Dupree C, Glogowska M, Case D, Antel JP, Owens GP, Gilden D, Nessler S, Stadelmann C, Hemmer B. Intrathecal pathogenic anti-aquaporin-4 antibodies in early neuromyelitis optica. Ann Neurol. 2009; 66(5):617–629. [PubMed: 19938104]
5. Botto M, Agnola CD, Bygrave AE, Thompson EM, Cook HT, Petry F, Loos M, Pandolfi PP, Walport MJ. Homozygous C1q deficiency causes glomerulonephritis associated with multiple apoptotic bodies. Nat Genet. 1998; 19:56–59. [PubMed: 9590289]
6. Botto M, Walport MJ. C1q, autoimmunity and apoptosis. Immunobiol. 2002; 205:395–406.
7. Crane JM, Lam C, Rossi A, Gupta T, Bennett JL, Verkman AS. Binding affinity and specificity of neuromyelitis optica autoantibodies to aquaporin-4 M1/M23 isoforms and orthogonal arrays. J Biol Chem. 2011; 286(18):16516–16524. [PubMed: 21454592]
8. Gadjeva MG, Rouseva MM, Zlatarova AS, Reid KBM, Kishore U, Kojouharova MS. Interaction of human C1q with IgG and IgM: revisited. Biochemistry. 2008; 47(49):13093–13102. [PubMed: 19006321]
9. Georgy MS, Pongracic JA. Chapter 22: hereditary and acquired angioedema. Allergy Asthma Proc. 2012; 33(Suppl 1):S73–S76. [PubMed: 22794695]
10. Ghai R, Waters P, Roumenina LT, Gadjeva M, Kojouharova MS, Reid KB, Sim RB, Kishore U. C1q and its growing family. Immunobiol. 2007; 212(4–5):253–266.
11. Gómez-Almaguer D. Monoclonal antibodies in the treatment of immune thrombocytopenic purpura (ITP). Hematology. 2012; 17(Suppl 1):S25–S27. [PubMed: 22507772]
12. Gomez AM, Van Den Broeck J, Vrolix K, Janssen SP, Lemmens MA, Van Der Esch E, Duimel H, Frederik P, Molenaar PC, Martínez-Martínez P, De Baets MH, Losen M. Antibody effector mechanisms in myasthenia gravis pathogenesis at the neuromuscular junction. Autoimmunity. 2010; 43:353–370. [PubMed: 20380584]
13. Greenberg BM, Graves D, Remington G, Hardeman P, Mann M, Karandikar N, Stuve O, Monson N, Frohman E. Rituximab dosing and monitoring strategies in neuromyelitis optica patients: creating strategies for therapeutic success. Mult Scler. 2012; 18(7):1022–1026. [PubMed: 22261118]
14. Hengstman GJ, Wesseling P, Frenken CW, Jongen PJ. Neuromyelitis optica with clinical and histopathological involvement of the brain. Mult Scler. 2007; 13(5):679–682. [PubMed: 17548452]
15. Hinson SR, McKeon A, Fryer JP, Apiwattanakul M, Lennon VA, Pittock SJ. Prediction of neuromyelitis optica attack severity by quantitation of complement-mediated injury to aquaporin-4-expressing cells. Arch Neurol. 2009; 66:1164–1167. [PubMed: 19752309]
16. Hinson SR, Pittock SJ, Lucchinetti CF, Roemer SF, Fryer JP, Kryzer TJ, Lennon VA. Pathogenic potential of IgG binding to water channel extracellular domain in neuromyelitis optica. Neurology. 2007; 69(24):2221–2231. [PubMed: 17928579]

17. Jacob A, McKeon A, Nakashima I, Sato DK, Elsone L, Fujihara K, de Seze J. Current concept of neuromyelitis optica (NMO) and NMO spectrum disorders. J Neurol Neurosurg Psych. 2013; 19:475–479.
18. Jarius S, Paul F, Franciotta D, Waters P, Zipp F, Hohlfeld R, Vincent A, Wildemann B. Mechanisms of disease: aquaporin-4 antibodies in neuromyelitis optica. Nat Clin Pract Neurol. 2008; 4(4):202–214. [PubMed: 18334978]
19. Jarius S, Wildemann B. AQP4 antibodies in neuromyelitis optica: diagnostic and pathogenetic relevance. Nature Rev Neurol. 2010; 6(7):383–392. [PubMed: 20639914]
20. Kieseier BC, Stüve O, Dehmel T, Goebels N, Leussink VI, Mausberg AK, Ringelstein M, Turowski B, Aktas O, Antoch G, Hartung HP. Disease amelioration with Tocilizumab in a treatment-resistant patient with neuromyelitis optica: implication for cellular immune responses. Arch Neurol. 2012; 24:1–4.
21. Kim SH, Kim W, Huh SY, Lee KY, Jung IJ, Kim HJ. Clinical efficacy of plasmapheresis in patients with neuromyelitis optica spectrum disorder and effects on circulating anti-aquaporin-4 antibody levels. J Clin Neurol. 2013; 9(1):36–42. [PubMed: 23346159]
22. Kira J. Autoimmunity in neuromyelitis optica and opticospinal multiple sclerosis: astrocytopathy as a common denominator in demyelinating disorders. J Neurol Sci. 2011; 311(1–2):69–77. [PubMed: 21962794]
23. Kishore U, Reid KBM. C1q: structure, function, and receptors. Immunopharmacol. 2000; 49:159–170.
24. Klos A, Tenner AJ, Johswich KO, Ager RR, Reis ES, Köhl J. The role of the anaphylatoxins in health and disease. Mol Immunol. 2009; 46(14):2753–2766. [PubMed: 19477527]
25. Kuroda H, Fujihara K, Takano R, Takai Y, Takahashi T, Misu T, Nakashima I, Sato S, Itoyama Y, Aoki M. Increase of complement fragment C5a in cerebrospinal fluid during exacerbation of neuromyelitis optica. J Neuroimmunol. 2013; 254(1–2):178–182. [PubMed: 23017732]
26. Lennon VA, Kryzer TJ, Pittock SJ, Verkman AS, Hinson SR. IgG marker of optic-spinal multiple sclerosis binds to the aquaporin-4 water channel. J Exp Med. 2005; 202(4):473–477. [PubMed: 16087714]
27. Lucchinetti CF, Mandler RN, McGavern D, Bruck W, Gleich G, Ransohoff RM, Trebst C, Weinshenker B, Wingerchuk D, Parisi JE, Lassmann H. A role for humoral mechanisms in the pathogenesis of Devic's neuromyelitis optica. Brain. 2002; 125(Pt 7):1450–1461. [PubMed: 12076996]
28. Mader S, Gredler V, Schanda K, Rostasy K, Dujmovic I, Pfaller K, Lutterotti A, Jarius S, Di Pauli F, Kuenz B, Ehling R, Hegen H, Deisenhammer F, Aboul-Enein F, Storch MK, Koson P, Drulovic J, Kristoferitsch W, Berger T, Reindl M. Complement activating antibodies to myelin oligodendrocyte glycoprotein in neuromyelitis optica and related disorders. J Neuroinflammation. 2011; 8:184. [PubMed: 22204662]
29. Manderson AP, Botto M, Walport MJ. The role of complement in the development of systemic lupus erythematosus. Annu Rev Immunol. 2004; 22:431–456. [PubMed: 15032584]
30. Misu T, Fujihara K, Kakita A, Konno H, Nakamura M, Watan-abe S, Takahashi T, Nakashima I, Takahashi H, Itoyama Y. Loss of aquaporin 4 in lesions of neuromyelitis optica: distinction from multiple sclerosis. Brain. 2007; 130(Pt 5):1224–1234. [PubMed: 17405762]
31. Nayak A, Pedneka L, Reid KB, Kishore U. Complement and non-complement activating functions of C1q: a prototypical innate immune molecule. Innate Immun. 2012; 18(2):350–363. [PubMed: 21450789]
32. Papadopoulos MC, Verkman AS. Aquaporin 4 and neuromyelitis optica. Lancet Neurol. 2012; 11(6):535–544. [PubMed: 22608667]
33. Parker C. Eculizumab for paroxysmal nocturnal haemoglo-binuria. Lancet. 2009; 373(9665):759–767. [PubMed: 19144399]
34. Phuan PW, Ratelade J, Rossi A, Tradtrantip L, Verkman AS. Complement-dependent cytotoxicity in neuromyelitis optica requires aquaporin-4 protein assembly in orthogonal arrays. J Biol Chem. 2012; 287(17):13829–13839. [PubMed: 22393049]

35. Pittock SJ, Lennon VA, McKeon A, Mandrekar J, Weinshenker BG, Lucchinetti CF, O'Toole O, Wingerchuk DM. Eculizumab in AQP4-IgG-positive relapsing neuromyelitis optica spectrum disorders: an open-label pilot study. Lancet Neurol. 2013 in press.
36. Ratelade J, Zhang H, Saadoun S, Bennett JL, Papadopoulos MC, Verkman AS. Neuromyelitis optica IgG and natural killer cells produce NMO lesions in mice without myelin loss. Acta Neuropathol. 2012; 123(6):861–872. [PubMed: 22526022]
37. Reff ME, Carner K, Chambers KS, Chinn PC, Leonard JE, Raab R, Newman RA, Hanna N, Anderson DR. Depletion of B cells in vivo by a chimeric mouse human monoclonal antibody to CD20. Blood. 1994; 83(2):435–445. [PubMed: 7506951]
38. Ricklin D, Hajishengallis G, Lambris JD. Complement: a key system for immune surveillance and homeostatis. Nat Immunol. 2010; 11(9):785–797. [PubMed: 20720586]
39. Ricklin D, Lambris JD. Progress and trends in complement therapeutics. Adv Exp Med Biol. 2013; 735:1–22. [PubMed: 23402016]
40. Risitano AM. Paroxysmal nocturnal hemoglobinuria and the complement system: recent insights and novel anticomplement strategies. Adv Exp Med Biol. 2013; 735:155–172. [PubMed: 23402025]
41. Roemer SF, Parisi JE, Lennon VA, Benarroch EE, Lassmann H, Bruck W, Mandler R, Weinshenker BG, Pittsock SJ, Wingerchuk DM, Lucchinetti CF. Pattern-specific loss of aquaporin-4 immunoreactivity distinguishes neuromyelitis optica from multiple sclerosis. Brain. 2007; 130(Pt 5):1194–1205. [PubMed: 17282996]
42. Saadoun S, Waters P, Bell BA, Vincent A, Verkman AS, Papadopoulos MC. Intra-cerebral injection of neuromyelitis optica immunoglobulin G and human complement produces neuromyelitis optica lesions in mice. Brain. 2010; 133(Pt 2):349–361. [PubMed: 20047900]
43. Saadoun S, Waters P, MacDonald C, Bell BA, Vincent A, Verkman AS, Papadopoulos MC. Neutrophil protease inhibition reduces neuromyelitis optica-immunoglobulin G-induced damage in mouse brain. Ann Neurol. 2012; 71(3):323–333. [PubMed: 22374891]
44. Sabater L, Giralt A, Boronat A, Hankiewicz K, Blanco Y, Llufriu S, Alberch J, Graus F, Saiz A. Cytotoxic effect of neuromyelitis optica antibody (NMO-IgG) to astrocytes: an in vitro study. J Neuroimmunol. 2009; 215:31–35. [PubMed: 19695715]
45. Sato D, Callegaro D, Lana-Peixoto MA, Fujihara K. Treatment of neuromyelitis optica: an evidence based review. Arq Neuropsiquiatr. 2012; 70(1):59–66. [PubMed: 22218475]
46. Schäfer MK, Schwaeble WJ, Post C, Salvati P, Calabresi M, Sim RB, Petry F, Loos M, Weihe E. Complement C1q is dramatically up-regulated in brain microglia in response to transient global cerebral ischemia. J Immunol. 2000; 164:5446–5452. [PubMed: 10799911]
47. Tam SH, Sassoli PM, Jordan RE, Nakada MT. Abciximab (ReoPro, chimeric 7E3 Fab) demonstrates equivalent affinity and functional blockade of glycoprotein IIb/IIIa and $\alpha_v\beta_3$ integrins. Circulation. 1998; 98(11):1085–1091. [PubMed: 9736595]
48. Tradtrantip L, Asavapanumas N, Verkman AS. Therapeutic cleavage of anti-aquaporin-4 autoantibody in neuromyelitis optica by an IgG-selective proteinase. Mol Pharmacol. 2013 in press.
49. Tradtrantip L, Ratelade J, Zhang H, Verkman AS. Enzymatic deglycosylation converts pathogenic neuromyelitis optica anti-aquaporin-4 immunoglobulin G into therapeutic antibody. Ann Neurol. 2013; 73(1):77–85. [PubMed: 23055279]
50. Tradtrantip L, Zhang H, Anderson MO, Saadoun S, Phuan PW, Papadopoulos MC, Bennett JL, Verkman AS. Small molecule inhibitors of NMO-IgG binding to aquaporin-4 reduce astro-cyte cytotoxicity in neuromyelitis optica. FASEB J. 2012; 26:2197–2208. [PubMed: 22319008]
51. Tradtrantip L, Zhang H, Saadoun S, Phuan PW, Lam C, Papadopoulos MC, Bennett JL, Verkman AS. Anti-aquaporin-4 monoclonal antibody blocker therapy for neuromyelitis optica. Ann Neurol. 2012; 71(3):314–322. [PubMed: 22271321]
52. Tüzün E, Li J, Saini SS, Yang H, Christadoss P. Targeting classical complement pathway to treat complement mediated autoimmune diseases. Adv Exp Med Biol. 2008; 632:265–272. [PubMed: 19025128]

53. Van Herle K, Behne JM, Van Herle A, Blaschke TF, Smith TJ, Yeaman MR. Integrative continuum: accelerating therapeutic advances in rare autoimmune diseases. Annu Rev Pharmacol Toxicol. 2012; 52:523–547. [PubMed: 22235861]
54. Vedove CD, Del Giglio M, Schena D, Girolomoni G. Drug-induced lupus erythematosus. Arch Dermatol Res. 2009; 301(1):99–105. [PubMed: 18797892]
55. Wallis R, Mitchell DA, Schmid R, Schwaeble WJ, Keeble AH. Paths reunited: initiation of the classical and lectin pathways of complement activation. Immunobiol. 2010; 215:1–11.
56. Wilde B, van Paassen P, Witzke O, Tervaert JW. New pathophysiological insights and treatment of ANCA-associated vasculitis. Kidney Int. 2011; 79:599–612. [PubMed: 21150876]
57. Wingerchuk DM. Neuromyelitis optica: potential roles for intravenous immunoglobulin. J Clin Immunol. 2013; 33(Suppl 1):S33–S37. [PubMed: 22976554]
58. Wingerchuk DM, Lennon VA, Lucchinetti CF, Pittock SJ, Wein-shenker BG. The spectrum of neuromyelitis optica. Lancet Neurol. 2007; 6(9):805–815. [PubMed: 17706564]
59. Wingerchuk DM, Lennon VA, Pittock SJ, Lucchinetti CF, Wein-shenker BG. Revised diagnostic criteria for neuromyelitis optica. Neurology. 2006; 66(10):1485–1489. [PubMed: 16717206]
60. Zipfel PF, Mihlan M, Skerka C. The alternative pathway of complement: a pattern recognition system. Adv Exp Med Biol. 2007; 598:80–92. [PubMed: 17892206]
61. Zipfel PF, Skerka C. Complement regulators and inhibitory proteins. Nature Rev Immunol. 2009; 9:729–740. [PubMed: 19730437]
62. Zhang H, Bennett JL, Verkman AS. Ex vivo spinal cord slice model of neuromyelitis optica reveals novel immunopathogenic mechanisms. Ann Neurol. 2011; 70(6):943–954. [PubMed: 22069219]
63. Zhang H, Verkman AS. Eosinophil pathogenicity mechanisms and therapeutics in neuromyelitis optica. J Clin Invest. 2013; 123(5):2306–2316. [PubMed: 23563310]

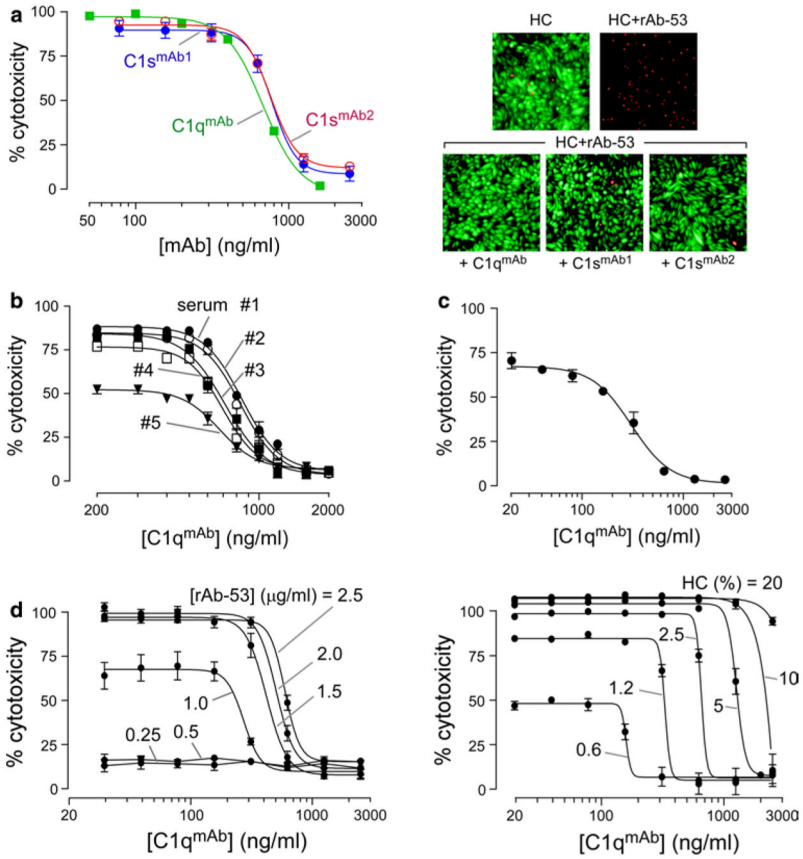

Fig. 1.

C1-targeted monoclonal antibodies prevent NMO-IgG-dependent, complement-dependent cytotoxicity (CDC). **a** (*left*) CDC in M23-AQP4-expressing CHO cells incubated for 60 min with 1.5 μg/ml rAb-53, 2 % human complement (HC), and $C1q^{mAb}$, $C1s^{mAb1}$ or $C1s^{mAb2}$ (S.E., *n* =4). (*right*) Live/dead (*green*/*red*) staining of cells incubated with 1.5 μg/ml rAb-53, 2 % HC and 2 μg/ml $C1q^{mAb}$, $C1s^{mAb1}$ or $C1s^{mAb2}$. **b** CDC in cells incubated with serum from five different NMO patients (2.5 %, heat-inactivated), 2 % HC and $C1q^{mAb}$ (S.E., *n* =4). **c** CDC in primary cultures of murine astrocytes incubated with 10 μg/ml rAb-53 (with CDC-enhancing mutation), 5 % HC and $C1q^{mAb}$ (S.E., *n* =4). **d** (*left*) CDC in M23-AQP4-expressing CHO cells incubated with 2 % HC and indicated concentrations of rAb-53 and $C1q^{mAb}$ (*left*, *n* =3). (*right*) CDC with 1.5 μg/ml rAb-53 and indicated concentrations of HC and $C1q^{mAb}$ (S.E., *n* =3)

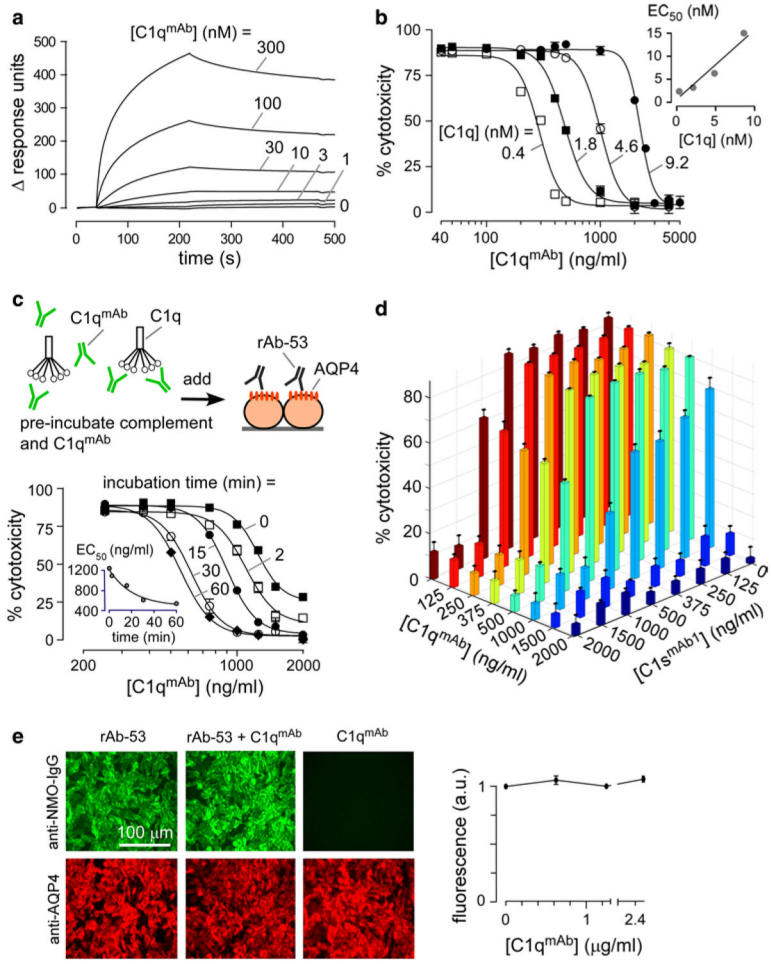

Fig. 2.

Characterization of C1q^{mAb}. **a** SPR sensorgram showing concentration-dependent binding of C1q^{mAb} to C1q. Purified C1q protein was ligated onto a CM5 sensor chip. C1q^{mAb} was injected for 180 s over the C1q followed by 300 s washout at a flow rate of 20 μl/min. **b** CDC in M23-AQP4-expressing CHO cells incubated with 1.5 μg/ml rAb-53, C1q^{mAb} and 2 % C1q-depleted serum containing indicated concentrations of purified human C1q protein. *Inset* shows EC_{50} vs. C1q concentration. **c** CDC in M23-AQP4-expressing CHO cells incubated with 1.5 μg/ml rAb-53, onto which was added a pre-incubated (for indicated times) mixture of C1q^{mAb} and 2 % HC. *Inset* shows apparent EC_{50} vs. time. **d** CDC assayed with 1.5 μg/ml rAb-53, 2 % HC and different concentrations of C1q^{mAb} and C1s^{mAb1} (S.E., *n* =3). **e** (*left*) M23-AQP4-expressing CHO cells were incubated with 1.5 μg/ml rAb-53 (immunostained *green*), shown with AQP4 immunofluorescence (*red*), with and without 2.5 μg/ml C1q^{mAb}. (*right*) rAb-53 binding to AQP4 in the presence of C1q^{mAb} measured using a Amplex Red HRP fluorescence assay

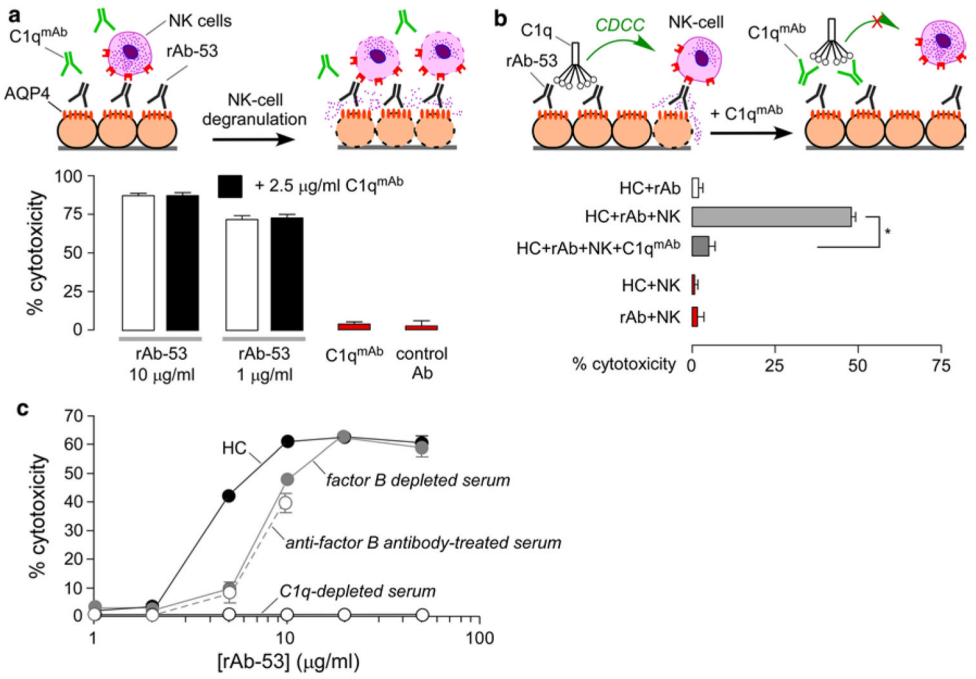

Fig. 3.

C1q^{mAb} prevents complement-dependent cell-mediated cyto-toxicity (CDCC) but not antibody-dependent cellular cytotoxicity (ADCC). **a** ADCC in M23-AQP4-expressing CHO cells incubated with 100,000 NK cells, 1 or 10 μg/ml rAb-53, with or without 2.5 μg/ml C1q^{mAb}. Controls included NK cells with C1q^{mAb} and rAb-2B4 (control antibody) alone (S.E., $n = 4$). **b** CDCC in M23-AQP4-expressing CHO cells incubated with 100,000 NK cells, 0.25 μg/ml rAb-53, 2.5 μg/ml C1q^{mAb} and 1 % HC. Controls included NK cells with 1 % HC and 0.25 μg/ml rAb-53 alone (S.E., $n = 4$, $^*p < 0.01$). **c** Amplification of cytotoxicity by the alternative complement pathway. M23-AQP4-expressing CHO cells incubated with rAb-53 together with 2 % HC, 2 % factor-B depleted human serum, or anti-factor B antibody-treated (100 μg/ml) HC (2 %). C1q-depleted serum with rAb-53 shown as control (S.E., n =4)

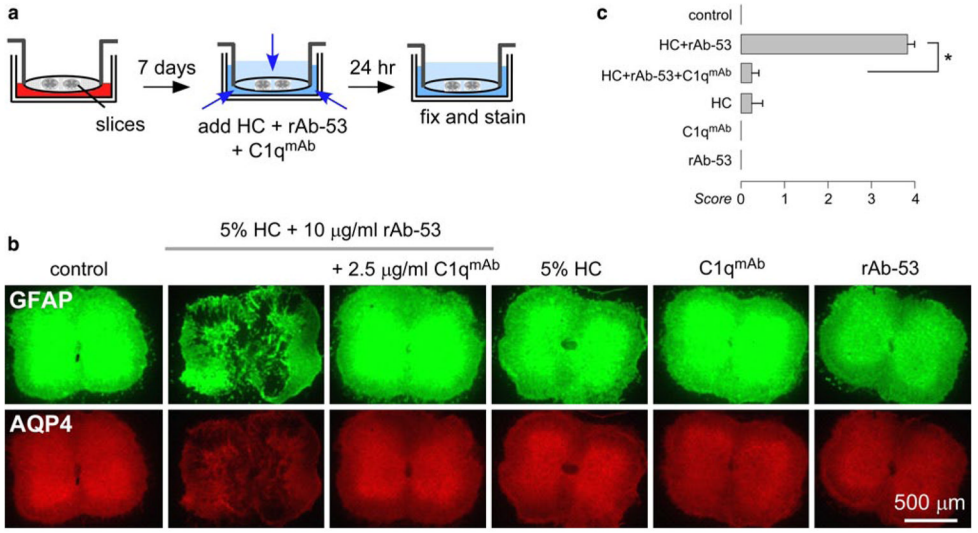

Fig. 4.

C1q^{mAb} prevents lesions in an ex vivo spinal cord slice mouse model of NMO. **a** Schematic of the spinal cord slice model of NMO. Mouse spinal cord slices were cultured for 7 days, followed by 24 h in the presence of 10 μg/ml rAb-53 and/or 5 % HC, with or without 2.5 μg/ml C1q^{mAb}. **b** Immunofluorescence of AQP4 (*red*) and GFAP (*green*). **c** NMO lesion scores (S.E., n =4–6, * p< 0.01)

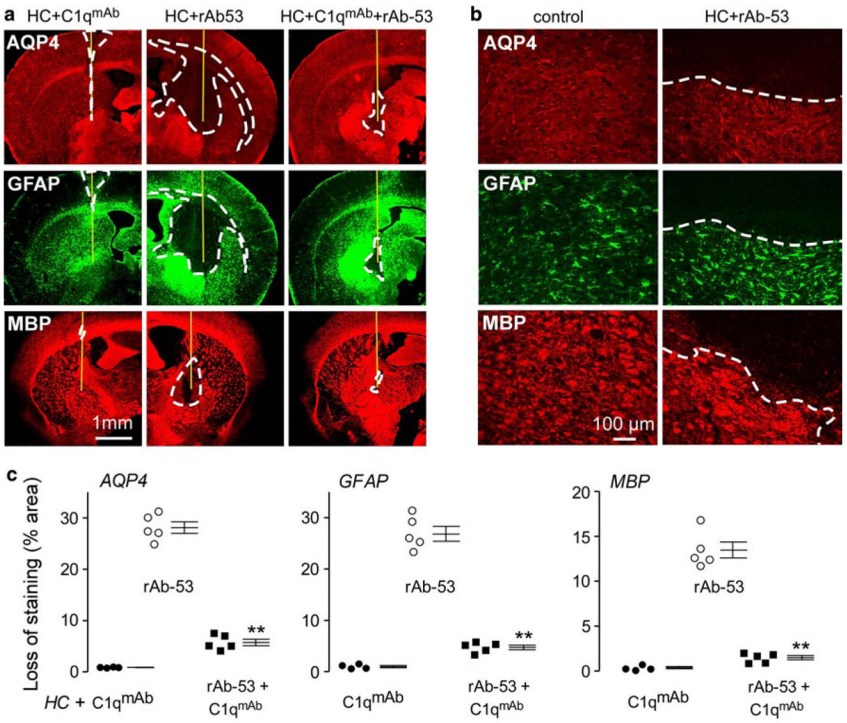

Fig. 5.

$C1q^{mAb}$ prevents lesions in an in vivo mouse model of NMO involving intracerebral injection of NMO antibody and complement. **a** Brains were injected with 3 μl HC and 1.3 μg $C1q^{mAb}$ (*left*), 0.9 μg rAb-53 (*middle*), and 0.9 μg rAb-53 + 1.3 μg $C1q^{mAb}$ (*right*). Representative GFAP, AQP4 and MBP immunofluorescence at 3 days after injection. *Yellow lines* represent the needle tract, and *white lines* delimit the lesion with loss of AQP4, GFAP, and myelin. **b** Higher magnification of brains injected with rAb-53 and HC. *White dashed lines* delimit the lesion. Contralateral (noninjected control) hemispheres are shown. **c** Summary of lesion size from experiments as in **a** (S.E., 4–5 mice per group, *$p < 0.01$)

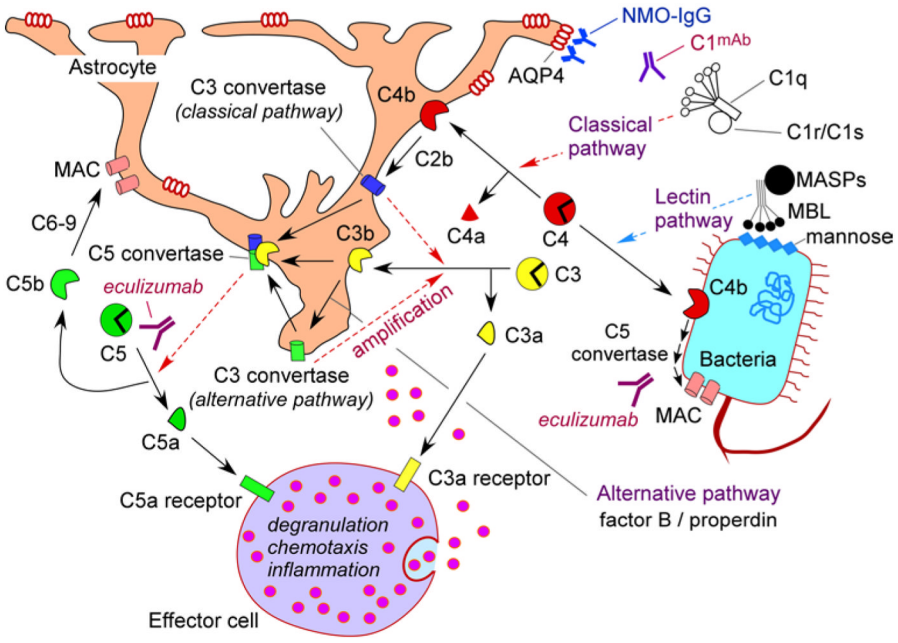

Fig. 6.

Schematic of complement pathways showing actions of C1q antibody in NMO pathogenesis. NMO-IgG binding to astrocyte AQP4 produces CDC through the classical pathway. Astrocyte damage is amplified by generation of C3a and C5a, which are involved in CDCC by causing effector cell chemot-axis, binding and degranulation, and by the alternative pathway. C1q inhibition prevents NMO-IgG dependent activation of the classical and alternative pathways, as well as CDCC. C5 inhibition by eculizumab prevents downstream complement activation through all complement pathways, including the lectin pathway. *MBL* mannose-binding lectin, *MASP* mannose-binding lectin-associated serine proteases